Tetrahedron 65 (2009) 232–239

Contents lists available at ScienceDirect

Tetrahedron

journal homepage: www.elsevier.com/locate/tet

Density functional theory rationalization of the substituent effects in trifluoromethyl-pyridinol derivatives

Jorge A. Fallas [a,†], Leticia González [b], Inés Corral [b,*]

[a] Institut für Chemie und Biochemie, Freie Universität Berlin, Takustraße 3, 14195 Berlin, Germany
[b] Institut für Physikalische Chemie, Friedrich-Schiller-Universität Jena, Helmholtzweg 4, 07743 Jena, Germany

ARTICLE INFO

Article history:
Received 4 September 2008
Received in revised form 21 October 2008
Accepted 21 October 2008
Available online 25 October 2008

Keywords:
Trifluoromethyl-pyridinol derivatives
Density functional theory calculations
Proton affinities
Gas phase basicities
Intramolecular hydrogen bonds

ABSTRACT

The influence of α-substitution in the structure, bonding and thermochemical properties of trifluoromethyl-pyridinol derivatives and their protonated counterparts has been studied by means of density functional theory. The geometries of the neutral and protonated species were optimized at the B3-LYP/6-311G(d,p) level of theory. Final energies were obtained through single point B3-LYP/6-311+G(3df,2p) calculations.

The relative orientation of the different substituents within the heterocycle ring favours the formation of unexpected intramolecular hydrogen bonds (IHB), which have been characterized by means of the Atoms in Molecules theory of Bader. Although weak, these IHB are of great importance for understanding the gas phase structure and the thermodynamical properties of these compounds. Surprisingly, most of the substituted investigated pyridinols present proton affinities below or close to that calculated for the unsubstituted pyridine molecule. Only pyridinols bearing strong σ or π donor activating groups show proton affinities greater than that of pyridine.

1. Introduction

Nitrogen heterocycles, such as pyridine derivatives, are commonly found in natural and synthetic products. Noticeable examples are the B_6 and B_2 vitamin families, which present as part of their structure, respectively, a pyridine nucleus[1] and a coenzyme nicotinamide adenine dinucleotide moiety containing in turn a pyridine-3-carboxamide[1] molecule.

The versatility of the pyridine heterocycle justifies its appearance as the repeating motif in many supramolecular structures with interesting photophysical, electrochemical and catalytic applications. A singular example is the case of 2,2′:6′,2″-terpyridine rhodium and copper complexes, which successfully catalyze biological reactions such as the reduction of NAD^+ into NADH[2] or the enantioselective cyclopropanation of styrene with diazoacetates.[3] Terpyridine metal compounds have also special interest as they can be used as synthons for the preparation of self-assembling supramolecular constructions with an a priori determined architecture, which renders specific electrochemical and spectroscopic properties.[4]

Functionalised pyridines are also widely used in therapeutics. A considerable number of antithrombus drugs,[5] antitumour[6–9] and antimicrobial agents[10–12] bear a pyridine heterocycle nucleus. Especially important for their pharmaceutical and agrochemical applications is the presence of the trifluoromethyl group, since fluorine atoms act as a powerful bioactive modulator. Despite their relevance, the characterization from the theoretical point of view of fluorine substituted pyridines is scarce.[13–17] In contrast, there is a large amount of papers reporting the synthesis of trifluoromethyl-substituted pyridines. For instance, Normansell and co-workers achieved the synthesis of pyridinedicarboxylated compounds through cyclocondensation of oxopentanedioates with trifluoroacetonitrile in the presence of sodium acetate or potassium *tert*-butoxide.[18] Twelve years later, Cottet and Schlosser[19] published the synthesis of trifluoromethyl-substituted pyridines through iodine displacement by (trifluoromethyl)copper. In 2003, the reaction of polyfluoroalkylchromones with dihydroisoquinolines to obtain diaryltrifluoroalkylpyridines was described by Shklyaev and co-workers.[20] A new synthesis of trifluoromethyl-pyridine derivatives has been reported by the group of Reißig in 2004.[21] Their paper describes the synthesis of trifluoromethyl-substituted pyridinol derivatives from the subsequent treatment of a nitrile (R–C≡N) with lithiated methoxyallene, trifluoroacetic acid and trimethylsilyl triflate. The coexistence of both the –OH and $–CF_3$ substituent groups within the pyridine molecule has special implications for constructing supramolecular organic structures with biological activity, as the hydroxyl group can be easily transformed into excellent leaving groups that are specially

* Corresponding author. Tel.: +49 3641 9 48336; fax: +49 3641 9 48302.
E-mail address: ines.corral@uni-jena.de (I. Corral).
† Present address: Department of Chemistry, Rice University, 6100 Main Street, Mail Stop 60, Houston, TX 77005, USA.

0040-4020/$ – see front matter © 2008 Elsevier Ltd. All rights reserved.
doi:10.1016/j.tet.2008.10.065

suited for undergoing palladium-catalyzed cross coupling reactions.

The aim of this paper is to characterize theoretically the neutral (**1**) and protonated (**1H**+) forms of the 3-methoxy-6-(trifluoromethyl)-4-pyridinol molecule, which constitutes a synthon for the construction of such biologically relevant systems. In order to learn more about this family of species, the structural and energetic changes induced upon α-substitution and their effect on the proton affinity (PA) were investigated. Our survey includes the unsubstituted compounds **1** and **1H**+, and the α-substituted compounds with R=CH_3 (compounds **2**, **2H**+), ^{t}Bu (**3**, **3H**+), Ph (**4**, **4H**+), F (**5**, **5H**+), NO_2 (**6**, **6H**+) and NH_2 (**7**, **7H**+) at position 2 (see Scheme 1).

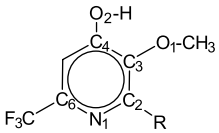

Scheme 1. Structure of 3-methoxy-6-(trifluoromethyl)-4-pyridinol derivatives considered in this study. R=–H, –CH_3, –^{t}Bu, –Ph, –F, –NO_2, –NH_2.

2. Computational details

The calculations were performed using the B3-LYP density functional, which includes Becke's three-parameter non-local hybrid exchange potential[22] and the non-local correlation functional of Lee, Yang and Parr.[23] For geometry optimizations, frequency calculations and thermochemical analysis, this functional was used in combination with a 6-311G(d,p) basis set. The corresponding harmonic vibrational frequencies and zero-point vibrational energies (ZPVE) were scaled by the empirical factors 0.9614 and 0.9806, respectively, recommended by Scott and Radom to account for anharmonicity effects.[24] Final energies were obtained through single point calculations using the 6-311+G(3df,2p) basis set. In order to assess the performance of the B3-LYP density functional in the description of neutral and cationic nitrogen heterocycles, selected structural, spectroscopic and thermochemical parameters were compared with those obtained using Møller Plesset second order perturbation theory[25] and with available experimental data (vide infra).

Natural Bond Orbital atomic population analysis[26] was used to explain certain structural features. This procedure has been proved to be more reliable than the Mulliken charge distribution scheme.[27]

The Atoms in Molecules (AIM) theory of Bader,[28] based on the description of the topology of the electronic density, was employed to characterize the nature of the species under study. In particular, the location of bond and ring critical points (bcp and rcp) is a very useful tool, which allows the identification of intramolecular hydrogen bonds (IHBs). Furthermore, the evaluation of the electronic density at these points provides a measure of the strength of these linkages.

All the calculations reported in this work have been carried out with the GAUSSIAN 03 series of programs.[29] The AIM 2000 software[30] was used for obtaining molecular graphs and for the analysis of the topology of the electronic density.

3. Results and discussion

3.1. Assessment of the theoretical procedure on pyridine

Even if nowadays the B3-LYP functional is the most common method chosen to undertake any theoretical study dealing with large systems, we find always sensible to calibrate the chosen protocol with an ab initio method for a test molecule; in this case we have chosen the pyridine molecule. The geometry and vibrational frequencies of pyridine obtained at B3-LYP/6-311G(d,p) level of theory were compared with those calculated at MP2/6-311G(d,p) as well as with the experimental data provided by Herzberg[31] and Klots.[32] Proton affinities (PA) and ionization potentials (IP) at B3-LYP/6-311+G(3df,2p) and MP2/6-311+G(3df,2p) are compared with the experimental values of Hunter and Lias.[33] All the experimentally available data and the obtained theoretical geometrical parameters, vibrational frequencies and selected relevant thermodynamic properties of pyridine are collected in Table 1.

It is gratifying to observe that the two sets of theoretical structures are in very good agreement with the experimental parameters. Deviations from the experiment in bond lengths and bond angles are less than ca. 0.01 Å and 1°, respectively. Also the empirically scaled B3-LYP and MP2 harmonic vibrational frequencies are very similar and in fairly good agreement with the experimental ones.[32] In general, the B3-LYP and MP2 stretching and bending normal modes are underestimated with respect to the experiment. The most noticeable deviations are registered for the symmetric CN stretching normal mode in the case of B3-LYP (29 cm^{-1}) and for the ring bending normal mode at MP2 level of theory (94 cm^{-1}). The deviation in the dipole moment is smaller for B3-LYP than for MP2. In the thermochemical analysis, we observe that B3-LYP provides a slightly better PA than MP2 compared to the experiment, while the opposite is observed for the IP. In any case, the deviation from the experimental PA (7.5 kJ/mol for B3-LYP and 10.4 kJ/mol for MP2) lies within the inherent error associated to the employed methods (5–10 kJ/mol).

In view of the overall excellent agreement between the experimental values and those obtained by B3-LYP and the chosen basis

Table 1
Experimental and optimized B3-LYP/6-311G(d,p) and MP2/6-311G(d,p) geometric parameters (Å and degrees), selected vibrational modes (cm^{-1}), and dipole moment (D), as well as B3-LYP/6-311+G(3df,2p) and MP2/6-311+G(3df,2p) thermochemical relevant properties (kJ/mol) for the pyridine molecule

Structure (distance in Å and angles in °)			
	Exp[30]	B3-LYP	MP2
$r(C_2–N_1)$	1.34	1.336 (1.350)[a]	1.343
$r(C_2–C_3)$	1.39	1.394 (1.381)[a]	1.398
$r(C_3–C_4)$	1.40	1.392 (1.396)[a]	1.396
$\angle(C_3C_2N_1)$	124.0	123.7	123.9
$\angle(C_6N_1C_2)$	116.7	117.2	116.7
$\angle(C_2C_3C_4)$	118.6	118.5	118.7
$\angle(C_3C_4C_5)$	118.1	118.5	118.2
$\angle(HC_2C_3)$	120.7	120.7	120.9
Harmonic vibrational frequencies (cm^{-1})			
	Exp[31]	B3-LYP	MP2
CH stretching (asym) B_2	3087	3062	3069
CH stretching (asym) B_2	3042	3022	3034
CH stretching (sym) A_1	1584	1563	1549
CN stretching (sym) A_1	1483	1454	1432
CH bending B_2	1442	1415	1397
Bending of the ring B_1	744	735	650
CH out of plane bending B_1	700	692	691
Thermochemical properties (dipole in D, PA and IP in kJ/mol)			
	Exp[32]	B3-LYP	MP2
Dipole moment	2.190	2.227	2.347
PA	930.01	937.51	919.61
IP	893.45	696.62	911.79

[a] B3-LYP/6-311G(d,p) geometrical parameters calculated for the pyridinium cation.

set, we now confidently proceed to characterize functionalised pyridines and their conjugated acids at this level of theory.

3.2. Structure and bonding of functionalised pyridines

The structures of the most stable conformers of 3-methoxy-6-(trifluoromethyl)-4-pyridinol derivatives and their corresponding protonated species are shown in Figure 1a and b, respectively. Some relevant molecular graphs are collected in Figure 2a and b. The red dots indicate the position of bcps and the yellow points symbolize rcps. The value of the electron density in e au^{-3} at the stationary points is also included to compare the strength of the molecular bonds.

Before discussing the effect of α-substitution in the structure of 3-methoxy-6-(trifluoromethyl)-4-pyridinol (**1**) and 3-methoxy-6-(trifluoromethyl)-4-pyridinium cation (**1H+**), we shall shortly analyze the changes induced by CF_3, OH and OCH_3 groups, common to all the species, in the bare pyridine and pyridinium cation skeletons.

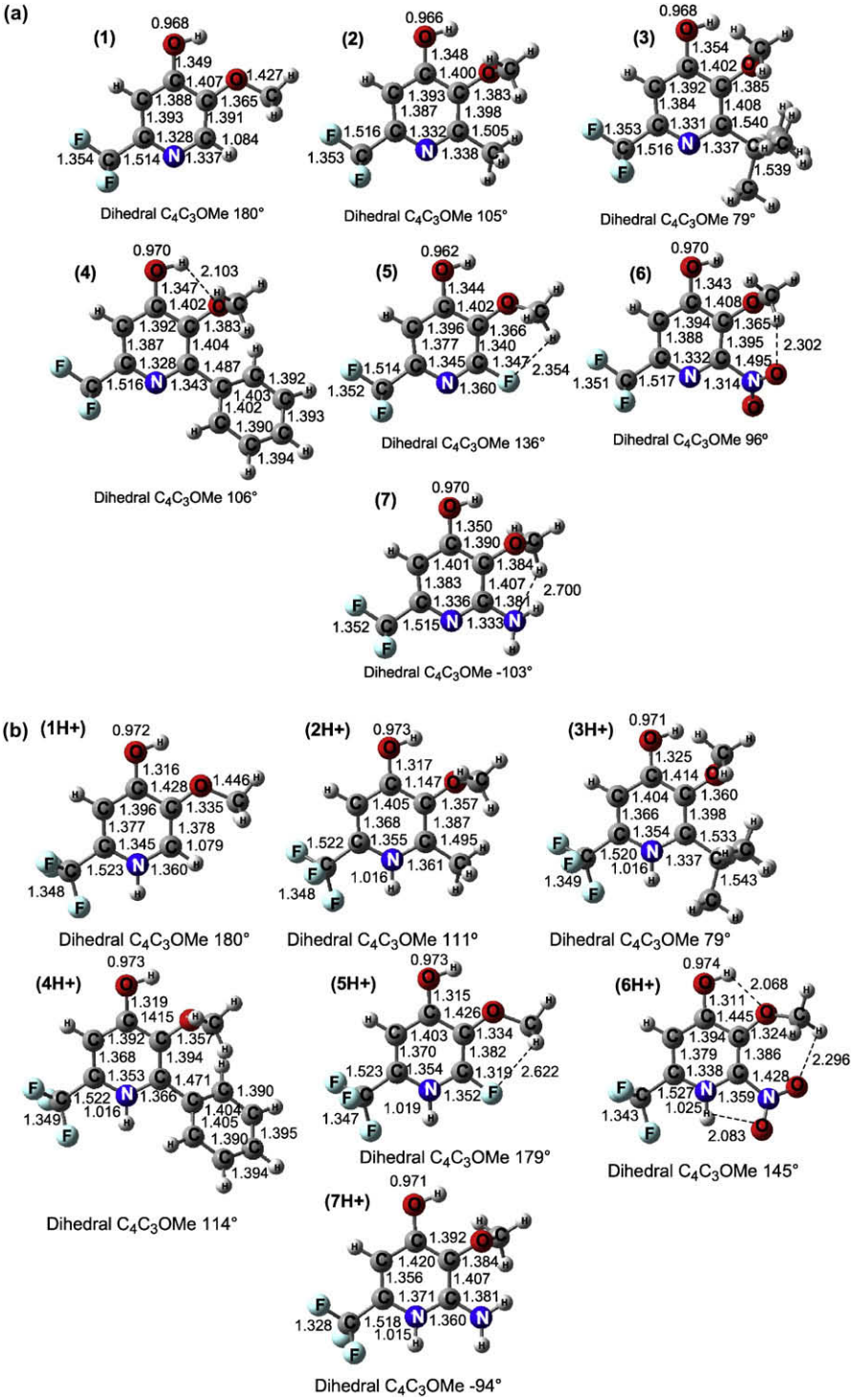

Figure 1. (a) B3-LYP/6-311G(d,p) optimized geometries of the most stable conformers of 3-methoxy-6-(trifluoromethyl)-4-pyridinol derivatives. Bond lengths in angstroms and bond angles in degrees. (b) B3-LYP/6-311G(d,p) optimized geometries of the most stable conformers of 3-methoxy-6-(trifluoromethyl)-4-pyridinium cation derivatives. Bond lengths in angstroms and bond angles in degrees.

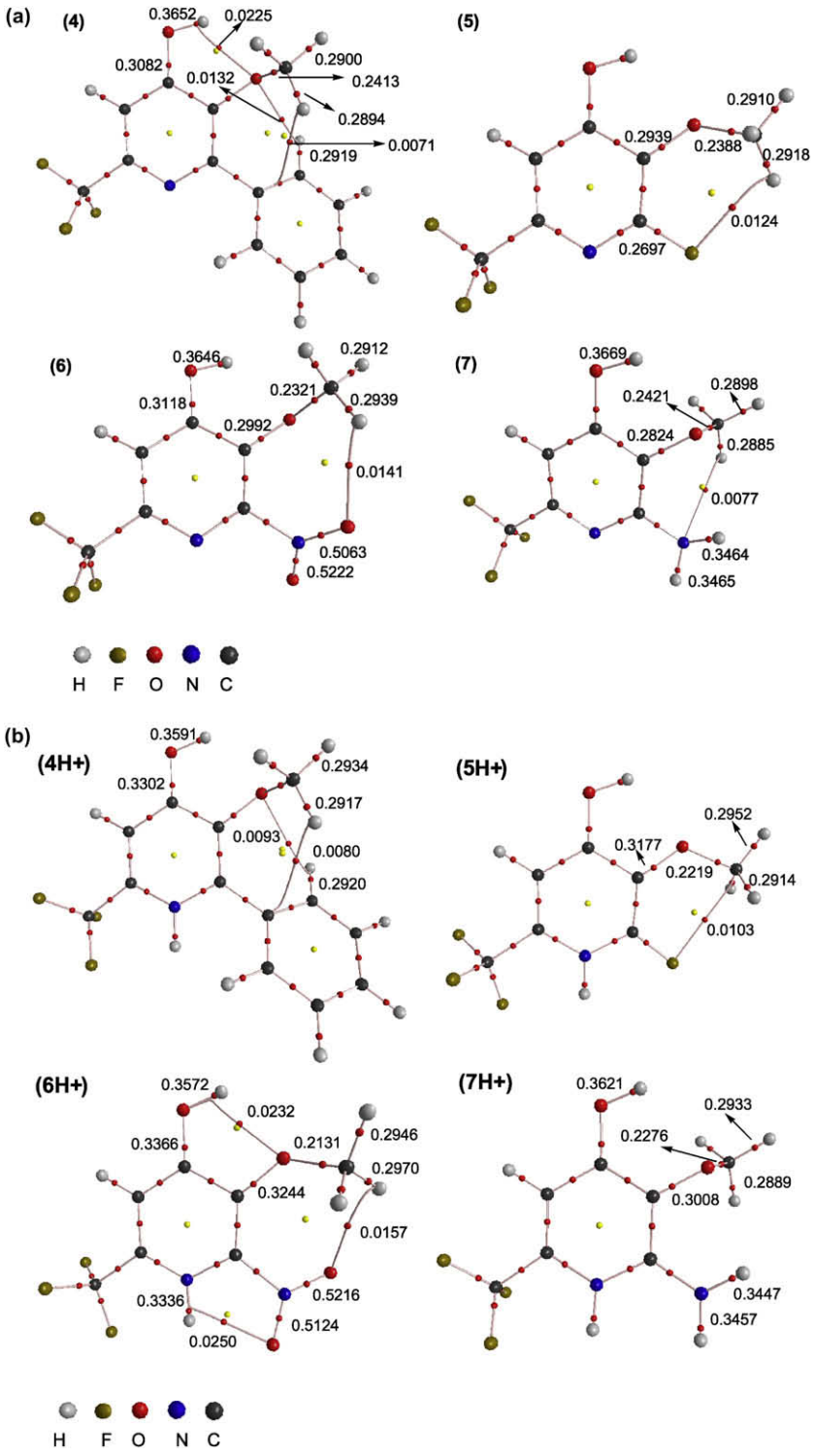

Figure 2. (a) Molecular graphs for **4**, **5**, **6** and **7** derivatives, showing the bond paths, the position of the bond critical points, ring critical points and the charge density (e au^{-3}) evaluated at these points at the B3-LYP/6-311G(d,p) level of theory. (b) Molecular graphs for **4H**+, **6H**+, **5H**+ and **7H**+ cation derivatives, showing the bond paths, the position of the bond critical points, ring critical points and the charge density (e au^{-3}) evaluated at these points at the B3-LYP/6-311G(d,p) level of theory.

To this aim, we compare the unprotonated and protonated structures **1** and **1H**+, in Figure 1a and b, respectively, with the structural parameters for the unsubstituted pyridine and pyridinium molecules, collected in Table 1. The net effect of the three substituents results in changes in the C_3–C_4 and N_1–C_6 bond distances (cf. Scheme 1), which weaken and reinforce, respectively, by ca. 0.015 and 0.01 Å in **1** and by 0.032 and 0.005 Å in **1H**+. The reinforcement of the N_1–C_6 bond adjacent to the trifluoromethyl group can be readily explained through the polarization exerted by the electron withdrawing group CF_3 on the C–N bond. On the other hand, the presence of two withdrawing groups attached to the C_3–C_4 bond is responsible of its weakening and consequent lengthening.

The changes on the common 3-methoxy-6-(trifluoromethyl)-4-pyridinol/pyridinium cation skeleton induced upon $-CH_3$, $-^tBu$,

Table 2
NBO net charges for all the calculated pyridinol derivatives and their conjugated acids

R=	–H (**1**)	$-CH_3$ (**2**)	$-^tBu$ (**3**)	–Ph (**4**)	–H (**1H**+)	$-CH_3$ (**2H**+)	^tBu (**3H**+)	–Ph (**4H**+)	–F (**5**)	$-NO_2$ (**6**)	$-NH_2$ (**7**)	–F (**5H**+)	$-NO_2$ (**6H**+)	$-NH_2$ (**7H**+)
C_2	−0.013	0.203	0.228	0.174	0.004	0.252	0.287	0.230	0.594	0.300	0.379	0.616	0.271	0.437
C_3	0.235	0.211	0.219	0.230	0.277	0.246	0.248	0.259	0.170	0.232	0.169	0.215	0.309	0.194
C_4	0.325	0.334	0.326	0.333	0.404	0.405	0.393	0.398	0.339	0.340	0.388	0.409	0.413	0.390
C_5	−0.264	−0.273	−0.268	−0.270	−0.241	−0.239	−0.235	−0.240	−0.271	−0.249	−0.298	−0.244	−0.240	−0.246
C_6	0.098	0.118	0.118	0.121	0.164	0.167	0.162	0.164	0.112	0.123	0.124	0.162	0.191	0.153
C_{CF_3}	1.078	1.079	1.079	1.079	1.090	1.090	1.090	1.090	1.078	1.078	1.079	1.090	1.091	1.091
F_{CF_3}	−0.354	−0.354	−0.355	−0.355	−0.354	−0.353	−0.353	−0.355	−0.352	−0.348	0.355	−0.352	−0.345	−0.356
C_{MeO}	−0.198	−0.195	−0.205	−0.198	−0.207	−0.196	−0.206	−0.198	−0.195	−0.202	−0.202	−0.197	−0.189	−0.202
N_1	−0.442	−0.446	−0.465	−0.458	−0.446	−0.463	−0.468	−0.458	−0.476	−0.426	−0.509	−0.495	−0.465	−0.505
O_1	−0.566	−0.597	−0.595	−0.600	−0.535	−0.576	−0.577	−0.577	−0.577	−0.584	−0.601	−0.534	−0.529	−0.585
O_2	−0.661	−0.662	−0.667	−0.661	−0.796	−0.599	−0.611	−0.604	−0.656	−0.651	−0.663	−0.594	−0.586	−0.610
X_R	0.197	−0.608	−0.124	−0.063	0.247	−0.626	−0.122	−0.110	−0.344	0.496	−0.749	−0.289	0.493	−0.739
H_{OH}	0.495	0.490	0.487	0.491	0.517	0.511	0.506	0.510	0.496	0.494	0.489	0.518	0.591	0.507
H_N	—	—	—	—	0.451	0.443	0.453	0.447	—	—	—	0.463	0.479	0.437

–Ph, –F, $-NO_2$ and $-NH_2$ α-substitution will be now analyzed by comparing the geometries of the different derivatives with those of **1** or **1H**+. These changes vary significantly with the substituent as a result of a complex interplay of the electron donor/acceptor ability and size of the substituent and the formation of IHBs in the derivatives.

The most significant structural change upon α-substitution occurs for the C_4C_3OMe dihedral, which has a value of 180° in the case of the reference compounds, the α-unsubstituted species, **1** and **1H**+. As expected, the biggest change in this dihedral angle is registered for the bulky ^{t}Bu derivatives (compounds **3** and **3H**+), where the methoxy group is forced to be almost perpendicular (dihedral 79°) to the ring plane in order to minimize the steric hindrance induced by the α-substituent. The same geometrical distortion can be found in species **2**, **4**, and **7** and their corresponding protonated species. Quite interestingly, this geometrical disposition allows for an IHB in the derivative **7**, involving the lone pair of the NH_2 group and a H of the methoxy group, see the corresponding bcp in Figure 2a. This IHB is very weak, with a bond length of 2.700 Å and an electron density at the bcp of ca. 0.008 e au^{-3}. The protonation of the pyridine heterocycle, however, leads to a change in the N_1C_2NH dihedral angle from 14.7° in the neutral to 4.8° in the protonated species, preventing the formation of an equivalent IHB in **7H**+. The absence of this IHB thus explains the 10° difference in the C_4C_3OMe dihedral angle between the **7** and **7H**+ amino species.

The methoxy group is also forced to be almost perpendicular to the pyridine plane in the nitro derivative **6**, but interestingly not after protonation, in **6H**+. This raises a pronounced difference in the C_4C_3OMe dihedral angle between them, compare 96.0° (**6**) versus 145.3° (**6H**+). The different conformation of the OMe group can be rationalized in view of the different number of IHB in which the methoxy group is involved in **6** and **6H**+. While in **6** the methoxy participates in one IHB, which also involves the NO_2 group (similar to the IHB found in **7**), in the protonated counterpart **6H**+, the methoxy group takes part in two different IHBs, the first with the NO_2 group and the second with the H of the OH group (see Fig. 2b). Additionally, a third IHB is present in **6H**+ involving the NO_2 group and the H of the pyridine heterocycle. It is the simultaneous participation of the methoxy group in more than one IHB, which forces the C_4C_3OMe dihedral angle near planarity in **6H**+. Worth highlighting is that the IHBs, which involve the pairs of substituents OMe/OH and NO_2/NH, are stronger than the one between the OMe and the NO_2 group. As can be taken from Figure 2b, the electron density associated with the former bcps (ca. 0.025 e au^{-3}) doubles that of the IHBs between the NO_2 and the OMe groups (ca. 0.014 e au^{-3} in both the **6** and **6H**+).

The fluorinated derivatives, **5** and **5H**+, also exhibit a marked difference in the C_4C_3OMe dihedral angle, **5** (136.3°) versus **5H**+ (179.4°), respectively, which can be as well attributed to the number of IHBs in each compound. In **5** there is only one IHB involving one hydrogen atom of the OMe group and the fluorine atom, see Figure 2a. The protonation of the pyridine ring, however, leads to the shortening of the C–F distance and a noticeable rearrangement of the CC distances inside the ring. As a result, the fluorine atom participates in two IHBs with two different hydrogens from the OMe group (see Fig. 2b), leading to a C_4C_3OMe dihedral angle close to 180°. As in other derivatives, the strength of the IHB both in **5** and **5H**+ is very weak, with electron densities at the bcp of the IHB ranging from 0.010 to 0.012 e au^{-3}.

Compound **4** gathers the largest number of IHB in its structure. The ability of the phenyl substituent to rotate around the C_3–$C_{benzene}$ axis provides enough flexibility to allow for the best arrangement of the OMe group, which participates in three IHBs: the first with the H of the OH group, the second with the C of the Ph substituent and the third with a H atom also from the Ph

Table 3
Selected scaled B3-LYP/6-311G(d,p) harmonic vibrational frequencies (cm^{-1}) of 3-methoxy-6-(trifluoromethyl)-4-pyridinol derivatives

R=	–H (**1**)	$-CH_3$ (**2**)	$-^tBu$ (**3**)	–Ph (**4**)	–F (**5**)	$-NO_2$ (**6**)	$-NH_2$ (**7**)
OH stretching	3616	3587	3675	3578	3589	3581	3598
CH_3 stretching (sym)	2900	2904	2909	2908	2918	2916	2906
CH_3 stretching (asym)	2962	2970	2992	2981	3029	3045	2974

substituent. The IHB between the OMe and the OH group (not occurring in **4H+**) presents the larger value of the electron density (0.023 e au^{-3}), resulting the strongest IHB among the three.

In the rest of the neutral and protonated species no IHB have been found even if the orientation of the hydrogen atom of the OH group facing the methoxy group is preferred due to the stabilizing electrostatic interaction established between these two atoms.

Bond distances are also affected upon α-substitution. For instance, excluding the fluorinated pyridinol (**5**), all the species under study show a weakening and concomitant lengthening of the C_2–C_3 distance with respect to **1** and **1H+**. This increase is connected to the size of the substituent. Thus, the biggest change is observed for R=^{t}Bu and R=Ph, where the bond lengthens by 0.017 and 0.013 Å in **3** and **4** and by 0.020 and 0.016 Å in **3H+** and **4H+**. In contrast, the small size of the fluorine atom together with its strong electron withdrawing character explain, not only that the C_2–C_3 distance does not increase, but even shortens due to a charge polarization process. Also directly related with the size of the substituents is the increase in the C_3–OMe distance upon α-substitution. As expected, the largest increase, ca. 0.020 Å, is found for the derivatives with the most voluminous substituents, that is, for R=Me, ^{t}Bu and Ph. Worth mentioning is also the weakening of the N_1–C_2 and N_1–C_6 bond distances upon fluorination (**5**), since both bonds are surrounded by strong electron withdrawing groups that are able to remove electron density from their bcps.

To conclude this section, other interesting differences between the neutral species and their protonated counterparts shall be pointed out, for example, the relative orientation of the CF_3 group with respect to the pyridine heterocycle. The unprotonated species favour an in-plane C–F bond lying trans with respect to the C–N bond of the heterocycle ring, whereas cis is found for the corresponding substituted pyridinium cations. The conformational preference of the CF_3 group can be explained by either the electrostatic destabilizing repulsion in the unprotonated species between the F and the N of the heterocycle ring, both bearing a negative charge, or the stabilizing attraction between the F and the H atom on the N atom in the protonated compounds (see Table 2). The only exception to this behaviour is **7**, which presents a non-planar FCC_6N dihedral angle of 34°. This slight rotation of the CF_3 substituent around the CC bond can be rationalized in terms of the partial NBO charges. This derivative presents the smallest positive partial charge on the hydrogen, which hence results in a less stabilizing electrostatic interaction that favours the out of plane deviation of the CF_3 group, see Table 2.

Other general changes also observed upon protonation of the heterocycle ring are the stretching of the C_2–N_1, C_6–N_1 bonds and the shortening of the C_4–OH and C_3–OMe bond distances. The weakening of the C_2–N_1 and C_6–N_1 bond distances is attributed to the electron withdrawing effect exerted by the proton on the N, whereas the changes in the C–O bond lengths find their origin in the polarization and electrostatic effects caused by the increase of the positive charge on C_3 and C_4 on going from the neutral to the protonated species, see Table 2.

3.3. Vibrational frequencies of functionalised pyridines

The most relevant vibrational frequencies of neutral and protonated substituted trifluoromethyl-pyridinols are tabulated in Tables 3 and 4, respectively. The most significant features concerning calculated infrared spectra (IR) of these species can be summarized as follows.

As observed in other fluorine containing systems,[34,35] the IR of trifluoromethyl-pyridinol compounds is dominated by bands arising from the C–F stretching normal modes in the region of 1200 cm^{-1}. This is due to the large dipole moment associated to the normal modes involving the F motion, which renders larger absorption coefficients and therefore greater intensities than those of C–C and C–H vibrations.

At higher energies, between 3500 and 3700 cm^{-1}, the IR spectra of the protonated pyrinidol derivatives are characterized by the typical very intense bands arising from NH and OH stretching normal modes.

The presence of IHBs is also imprinted in the IR spectra. Compound **4** presents the smallest O–H stretching frequency, 3578 cm^{-1}, due to the participation of the hydroxyl group in a quite strong IHB. This is also the case in **6H+** whose O–H and N–H stretching vibrational frequencies appear 30 cm^{-1} and 114 cm^{-1} redshifted compared to **1H+**, due to the participation of the OH and NH bonds into two IHBs (see Table 4). In contrast, small blue shifts of the C–H harmonic stretching vibrational frequencies were found in the derivatives containing the very weak IHB, which involve the –OMe group, compare the symmetric and asymmetric CH_3 stretching vibrational frequencies in the –F and $-NO_2$ derivatives with the rest of compounds. Such counterintuitive blue shift was previously reported for a number of improper H-bonded complexes, such as carbon proton donor benzene,[36] the chloroform–benzene[37] and Z–X–H···Y[38] (where X is not necessarily an electronegative atom) complexes and was attributed either to a charge transfer from the proton acceptor to a remote part of the proton donor molecule[39] or to an intramolecular charge transfer, which increases the electronegativity of the X atom contracting the X–H bond distance.[38]

3.4. Proton affinities and gas phase basicities of functionalised pyridines

Proton affinity (PA) and gas phase basicity (GB) are fundamental gas phase thermodynamic properties. Most of the experimental

Table 4
Selected scaled B3-LYP/6-311G(d,p) harmonic vibrational frequencies (cm^{-1}) of 3-methoxy-6-(trifluoromethyl)-4-pyridinium cation derivatives

R=	–H (**1H+**)	$-CH_3$ (**2H+**)	$-^tBu$ (**3H+**)	–Ph (**4H+**)	–F (**5H+**)	$-NO_2$ (**6H+**)	$-NH_2$ (**7H+**)
NH stretching	3410	3404	3394	3402	3384	3296	3419
OH stretching	3566	3543	3581	3540	3555	3536	3581
CH_3 stretching (sym)	2921	2930	2930	2933	2946	2953	2924
CH_3 stretching (asym)	2998	3008	3006	3016	3032	3048	2998

Table 5
Proton affinities (PA, kJ/mol) and gas phase basicities (GB, kJ/mol) of 3-methoxy-6-(trifluoromethyl)-4-pyridinol derivatives

R=	PA (kJ/mol)	GB (kJ/mol)
–H (**1**)	929.17	893.99
$-CH_3$ (**2**)	936.24	902.02
$-^tBu$ (**3**)	943.89	910.85
–Ph (**4**)	950.04	914.28
–F (**5**)	884.40	849.83
$-NO_2$ (**6**)	877.87	843.81
$-NH_2$ (**7**)	932.69	897.26

GBs values available in the literature are obtained from equilibrium constant measurements involving proton transfer reactions. However, obtaining absolute PA values is not straightforward due to the experimental difficulties in measuring the equilibrium constant as a function of the temperature to estimate the entropy change. Table 5 summarizes the calculated PAs and GBs for the title compounds.

The first striking fact is that the unsubstituted pyridinol molecule, R=H, presents a PA 8 kJ/mol smaller than the bare pyridine. This is quite unexpected as the presence of two substituents regarded as strong and moderate π-donors, OH and OCH_3, should increase the PA with respect to the pyridine. However, the orientation of the hydroxyl and methoxy group in the neutral system prevents from an effective overlap between their orbitals and those of the heterocycle ring difficulting the charge transfer from the π-donors substituents to the ring. This, summed up to the effect of the strong σ-acceptor group, CF_3, counteracts the increased polarization component created by the substituents and results in a reduced PA.

The same arguments can be recalled to explain the lower than expected PA of **7**. On the one hand side, the electron withdrawing effect of the CF_3 group cancels the polarization contribution, and on the other hand, the poor overlap of the p-orbital of the nitrogen with the π orbitals of the ring disrupts the π-donation. As a result, the PA of **7** is also decreased as compared to that of pyridine.

In contrast, the derivatives containing σ-donor substituents, like the methyl and *tert*-butyl group, show greater PAs than the unsubstituted pyridinol. Here, the effect of the polarization component, directly related to the size of the substituent, is nicely reflected in the change of the PA on going from the smaller substituents ($-CH_3$) to the most voluminous one (–Ph). In this respect, the PA of **2** is 7 kJ/mol greater than that of **1**, but 8 kJ/mol smaller than the one calculated for **3**. Naturally, the biggest PA is found for R=Ph. In addition to the strong polarization component associated to the size and the σ-donor ability of the –Ph substituent, it constitutes a weakly π-activating group able to transfer some charge into the heterocycle through orbital overlapping.

As expected, the deactivating nitro and fluorine substituted derivatives show the smallest PA among all the derivatives studied. In summary, the PA scale for the studied compounds is the following:

PA(**6**)<PA(**5**)<PA(**1**)<PA(**7**)<PA(**2**)<PA(**pyridine**)<PA(**3**)<PA(**4**)

4. Conclusions

The structure, bonding and energetics of substituted trimethylpyridinols and their protonated counterparts have been studied by means of density functional methods. An analysis of the topology of the electron density revealed the existence of weak intramolecular hydrogen bonds, which in many cases involve the electronegative atom of the substituents and the H of the methoxy group or the proton in position 1 from the N heterocycle. The ability to form different hydrogen bond networks heavily influences the structure of the neutral versus the protonated compounds. Due to their weakness, the normal modes associated to the atoms involved in the hydrogen bonds do not appear significantly redshifted in the IR spectra, which are otherwise mainly dominated by vibrational bands involving C–F stretching normal modes.

Also important is the effect of the CF_3 group in the values of the proton affinities and gas basicities for the studied compounds. The substitution of the hydrogen atom in position 2 by alkyl groups, such as $-CH_3$ and $-^tBu$, results in a moderate increase around 5–15 kJ/mol in the proton affinities. The relative orientation of the π donor substituents, –OH and –OMe, with respect to the plane of the heterocycle ring prevents from an adequate orbital overlapping and therefore the charge transfer from the substituents is greatly reduced. These effects result in proton affinities close to that of the bare pyridine heterocycle. Stronger deactivating groups such as NO_2 and fluorine atom are able to decrease the proton affinity up to 50 kJ/mol. The largest proton affinity, 950 kJ/mol, was found for the phenyl containing derivative, yet only 13 kJ/mol bigger than that calculated for the pyridine molecule.

Acknowledgements

The authors wish to thank H.-U. Reißig (Berlin) and the SFB 765 for stimulating this study. Financial support from the 'Fundación Ramón Areces' (I.C.), the 'Humboldt Stiftung' (I.C.) and 'Berliner Frauenförder Programm' (L.G.) at the time this research was performed is also gratefully acknowledged. The calculations have been done in the HP workstations at the Theoretical Chemistry Group at the Freie Universität Berlin and the Friedrich-Schiller Universität Jena.

References and notes

1. Gilchrist, T. L. *Heterocyclic Chemistry*; John Wiley & Sons: New York, NY, 1988.
2. Umeda, K.; Nakamura, A.; Toda, F. *Bull. Chem. Soc. Jpn.* **1993**, *66*, 2260.
3. Chelucci, G.; Saba, A.; Soccolini, F.; Vignola, D. *J. Mol. Catal. A: Chem.* **2002**, *178*, 27.
4. Díaz, D. J.; Bernhard, S.; Storrier, D.; Abruña, H. D. *J. Phys. Chem. B* **2001**, *105*, 8746.
5. Altenburger, J. M.; Lassalle, G. Y.; Matrougui, M.; Galtier, D.; Jetha, J. C.; Bocskei, Z.; Berry, C. N.; Lunven, C.; Lorrain, J.; Herault, J. P.; Schaeffer, P.; O'Connor, S. E.; Herbert, J. M. *Bioorg. Med. Chem.* **2004**, *12*, 1713.
6. Mason, D. N.; Deacon, G. B.; Yellowlees, L. J.; Bond, A. M. *Dalton Trans.* **2003**, *5*, 890.
7. Kovala-Demertzi, D.; Demertzis, M. A.; Miller, J. R.; Papadopoulou, C.; Dodorou, C.; Filousis, G. *J. Inorg. Biochem.* **2001**, *86*, 555.
8. Julino, M.; Stevens, M. F. G. *J. Chem. Soc., Perkin Trans. 1* **1998**, 1677.
9. Amr, A. G. E.; Mohamed, A. M.; Mohamed, S. F.; Abdel-Hafez, N. A.; Hammam, A. *Bioorg. Med. Chem.* **2006**, *14*, 5481.
10. Zhuravel, I. O.; Kovalenko, S. M.; Ivachtchenko, A. V.; Balakin, K. V.; Kazmirchuk, V. V. *Bioorg. Med. Chem. Lett.* **2005**, *15*, 5483.
11. Bakhite, E. A.; Al-Sehemi, A. G.; Yamada, Y. *J. Heterocycl. Chem.* **2005**, *42*, 1069.
12. Elkholy, Y. M. *Heterocycl. Commun.* **2005**, *11*, 89.
13. Lichter, R. L.; Wasylishen, R. E. *J. Am. Chem. Soc.* **1975**, *97*, 1808.
14. Dewar, M. J. S.; Yamaguchi, Y.; Doraiswamy, S.; Sharma, S. D.; Suck, S. H. *Chem. Phys.* **1979**, *41*, 21.
15. Fraenk, W.; Klapotke, T. M.; Banks, E.; Besheesh, M. K. *J. Fluorine Chem.* **2001**, *108*, 87.
16. Barone, V.; Peralta, J. E.; Contreras, R. H.; Snyder, J. P. *J. Phys. Chem. A* **2002**, *106*, 5607.
17. Hou, X. J.; Huang, M. B. *Chin. J. Chem. Phys.* **2004**, *17*, 143.
18. Lee, L. F.; Normansell, J. E. *J. Org. Chem.* **1990**, *55*, 2964.
19. Cottet, F.; Schlosser, M. *Eur. J. Org. Chem.* **2002**, 327.
20. Sosnovskikh, V. Y.; Usachev, B. I.; Sizov, A. Y.; Vorontsov, I. I.; Shklyaev, Y. V. *Org. Lett.* **2003**, *5*, 3123.
21. Flögel, O.; Dash, J.; Brüdgam, I.; Hartl, H.; Reißig, H.-U. *Chem.—Eur. J.* **2004**, *10*, 4283.
22. Becke, A. D. *J. Chem. Phys.* **1993**, *98*, 1372.
23. Lee, C.; Yang, W.; Parr, R. G. *Phys. Rev. B: Condens. Matter* **1988**, *37*, 785.
24. Scott, A. P.; Radom, L. *J. Phys. Chem.* **1996**, *100*, 16502.
25. Møller, C.; Plesset, M. S. *Phys. Rev.* **1934**, *46*, 618.
26. Reed, A. E.; Weinstock, R. B.; Weinhold, F. *J. Chem. Phys.* **1985**, *83*, 735.
27. Mulliken, R. S. *J. Chem. Phys.* **1955**, *23*, 1833.
28. Bader, R. F. W. *Atoms in Molecules. A Quantum Theory*; Oxford University Press: USA, 1990.
29. Frisch, M. J.; Trucks, G. W.; Schlegel, H. B.; Scuseria, G. E.; Robb, M. A.; Cheeseman, J. R.; Montgomery, J. A., Jr.; Vreven, T.; Kudin, K. N.; Burant, J. C.;

Millam, J. M.; Iyengar, S. S.; Tomasi, J.; Barone, V.; Mennucci, B.; Cossi, M.; Scalmani, G.; Rega, N.; Petersson, G. A.; Nakatsuji, H.; Hada, M.; Ehara, M.; Toyota, K.; Fukuda, R.; Hasegawa, J.; Ishida, M.; Nakajima, T.; Honda, Y.; Kitao, O.; Nakai, H.; Klene, M.; Li, X.; Knox, J. E.; Hratchian, H. P.; Cross, J. B.; Adamo, C.; Jaramillo, J.; Gomperts, R.; Stratmann, R. E.; Yazyev, O.; Austin, A. J.; Cammi, R.; Pomelli, C.; Ochterski, J. W.; Ayala, P. Y.; Morokuma, K.; Voth, G. A.; Salvador, P.; Dannenberg, J. J.; Zakrzewski, V. G.; Dapprich, S.; Daniels, A. D.; Strain, M. C.; Farkas, O.; Malick, D. K.; Rabuck, A. D.; Raghavachari, K.; Foresman, J. B.; Ortiz, J. V.; CuiA, Q.; Baboul, G.; Clifford, S.; Cioslowski, J.; Stefanov, B. B.; Liu, G.; Liashenko, A.; Piskorz, P.; Komaromi, I.; Martin, R. L.; Fox, D. J.; Keith, T.; Al-Laham, M. A.; Peng, C. Y.; Nanayakkara, A.; Challacombe, M.; Gill, P. M. W.; Johnson, B.; Chen, W.; Wong, M. W.; Gonzalez, C.; Pople, J. A.; *Gaussian 03, Revision D.01*; Gaussian: Wallingford, CT, 2004.

30. Biegler-König, F.; Bayles, D.; Schönbohm, J. *AIM2000, version 1.0*; University of Applied Sciences: Bielefeld, Germany, 2000.
31. Herzberg, G. *Electronic Spectra and Electronic Structure of Polyatomic Molecules*; Van Nostrand: New York, NY, 1966.
32. Klots, T. D. *Spectrochim. Acta, Part A* **1998**, *54*, 1481.
33. Hunter, E. P.; Lias, S. G. *J. Phys. Chem. Ref. Data* **1998**, *27*, 413.
34. Crowder, G. A.; Koger, T. *J. Mol. Struct.* **1975**, *29*, 233.
35. Crowder, G. A.; Mao, H.-K. *J. Mol. Struct.* **1974**, *23*, 161.
36. Hobza, P.; Spirko, V.; Selzle, H. L.; Schlag, E. W. *J. Phys. Chem. A* **1998**, *102*, 2501.
37. Hobza, P.; Spirko, V.; Havlas, Z.; Buchhold, K.; Reinmann, B.; Barth, H.-D.; Brutschy, B. *Chem. Phys. Lett.* **1999**, *299*, 180.
38. Kolandaivel, P.; Nirmala, V. *J. Mol. Struct.* **2004**, *694*, 33.
39. Müller-Dethlefs, K.; Hobza, P. *Chem. Rev.* **2000**, *100*, 143.